

# HGIB: Prognosis for Alzheimer’s Disease via Hypergraph Information Bottleneck

Shujun Wang<sup>1</sup>, Angelica I Aviles-Rivero<sup>1</sup>, Zoe Kourtzi<sup>2</sup>, and Carola-Bibiane Schönlieb<sup>1</sup>

<sup>1</sup> DAMTP, University of Cambridge, Cambridge, UK  
{sw991, ai323, cbs31}@cam.ac.uk

<sup>2</sup> Department of Psychology, University of Cambridge, Cambridge, UK  
zk240@cam.ac.uk

**Abstract.** Alzheimer’s disease prognosis is critical for early Mild Cognitive Impairment patients for timely treatment to improve the patient’s quality of life. Whilst existing prognosis techniques demonstrate potential results, they are highly limited in terms of using a single modality. Most importantly, they fail in considering a key element for prognosis: not all features extracted at the current moment may contribute to the prognosis prediction several years later. To address the current drawbacks of the literature, we propose a novel hypergraph framework based on an information bottleneck strategy (**HGIB**). Firstly, our framework seeks to discriminate irrelevant information, and therefore, solely focus on harmonising relevant information for future MCI conversion prediction (*e.g.*, two years later). Secondly, our model simultaneously accounts for multi-modal data based on imaging and non-imaging modalities. HGIB uses a hypergraph structure to represent the multi-modality data and accounts for various data modality types. Thirdly, the key of our model is based on a new optimisation scheme. It is based on modelling the principle of information bottleneck into loss functions that can be integrated into our hypergraph neural network. We demonstrate, through extensive experiments on ADNI, that our proposed HGIB framework outperforms existing state-of-the-art hypergraph neural networks for Alzheimer’s disease prognosis. We showcase our model even under fewer labels. Finally, we further support the robustness and generalisation capabilities of our framework under both topological and feature perturbations.

**Keywords:** Prognosis prediction · Alzheimer’s disease · Hypergraph · Information bottleneck · Multi-modality data

## 1 Introduction

Alzheimer’s disease (AD) is a progressive and irreversible neurodegenerative disorder that results in a high level of dependence. The disease progresses through different stages, starting with Mild Cognitive Impairment (MCI), characterized by memory problems, and eventually leading to AD. However, not all patients diagnosed with MCI convert to Alzheimer’s disease, and some may remain stable

or even revert to normal. This distinction between MCI stablers, MCI progressors, and MCI non-converters highlights the need for accurate prognosis prediction. Although there is no known cure for AD, the development of algorithmic techniques for prognosis has attracted great interest from the medical community. Early treatment for MCI progress is crucial for improving patients’ quality of life, making the value of accurate prognosis prediction evident.

The literature has extensively investigated the task of predicting MCI to AD conversion from various perspectives. Early studies focused on analyzing a region of interest [3,5,15], different single modalities or neuropsychological evaluation [6, 19,20], and informative AD biomarkers [11,21]. These have been widely explored using support vector machines (SVM) alone or in combination with Gaussian Radial functions [14, 26]. With the advent of deep learning, researchers have explored the use of convolutional neural networks (CNNs) for MCI conversion prediction employing transfer learning and pyramid networks [2, 17, 22, 24, 28].

Although there have been promising results in MCI conversion prediction in the literature, there are two major drawbacks that limit their performance. Firstly, existing techniques mainly rely on a single modality, which may not capture the full picture of the disease progression. To address this, recent studies have emphasized the need to develop multi-modal techniques that can extract richer information [1, 10, 23]. Secondly, how to effectively extract discriminative information from the multi-modal data to facilitate conversion prediction and discard the irrelevant information from high heterogeneity multi-modality data has not been explored in the existing literature yet.

In this work, we propose a novel approach, namely the hypergraph information bottleneck strategy (HGIB), to address the existing limitations in Alzheimer’s disease prognosis leveraging multi-modality data. HGIB utilises a hypergraph structure to represent the multi-modal features and harmonises various modality data types. In contrast to existing techniques, HGIB focuses on learning discriminative representations that are meaningful with minimal but relevant information, by applying the principle of information bottleneck. *To the best of our knowledge, this is the first hypergraph framework specifically designed for prognosis rather than diagnosis.* Experiments on the public ADNI dataset for Alzheimer’s disease prognosis prediction demonstrate that HGIB outperforms other state-of-the-art hypergraph neural network architectures in supervised learning settings as well as with fewer annotations. Additionally, HGIB exhibits robustness against topological and feature perturbations, highlighting its potential for future research in this field.

## 2 Proposed Framework

This section presents a detailed description of the crucial components of our proposed framework. Firstly, we elucidate the process of constructing the hypergraph from a given set of multi-modal data, and we delve into the specifics of the hypergraph convolution definition. Secondly, we explicate the fundamental principle of information bottleneck and integrate it into hypergraph neural networks. The overview of the proposed method is illustrated in Fig. 1.

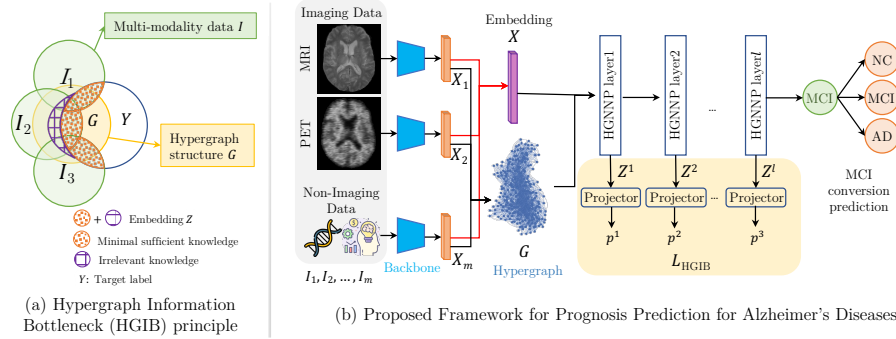


**Fig. 1.** Illustration of the whole workflow. (a) shows how hypergraph information bottleneck utilised to optimize the representation  $Z$  to capture the minimal sufficient information within the input data  $D = (G, I)$  to predict the MCI conversion label  $Y$ . (b) is the overall workflow integrating HGIB into the hypergraph neural network. HGNNP is a kind of hypergraph convolutional layer.

## 2.1 Hypergraph Modelling and Hypergraph Convolution

To overcome the challenges associated with multi-modality data  $(I_1, I_2, \dots, I_m)$ , we leverage a hypergraph structure  $G$  to represent the multi-modal features  $(X_1, X_2, \dots, X_m)$  extracted from backbones. Subsequently, we employ a hypergraph neural network to predict MCI conversion.

**Hypergraph representation learning.** We consider an undirected attributed hypergraph  $G = (V, E, \mathbf{H})$  with a vertex set  $V$ , a hyperedge set  $E$ , and an adjacency matrix  $\mathbf{H} \in \mathbb{R}^{|V| \times |E|}$  for hyperedge weight. Each vertex in our hypergraph structure corresponds to a patient, while each hyperedge represents the relationship between a subset of vertices. Unlike in a graph structure, where an edge connects only two vertices, a hyperedge in a hypergraph connects multiple vertices, enabling the representation of higher-order relationships. This feature facilitates the grouping of subsets of vertices with common features or properties, enhancing the ability of the hypergraph to model complex relationships within the data. In our hypergraph structure, each vertex corresponds to a patient and each hyperedge represents the relationship between a subset of the vertices. Unlike in a graph structure, a hyperedge in a hypergraph connects multiple vertices instead of just two, allowing for the representation of higher-order relationships. This can be seen as the hyperedges grouping together subsets of vertices that have common features or properties. Specifically, the hyperedge weight between vertex  $v$  and hyperedge  $e$  can be defined as  $h_{v,e} = \begin{cases} 1 & \text{if } v \in e \\ 0 & \text{otherwise} \end{cases}$ . Moreover, we denote the vertex attributes as  $X$ , which can be seen as a feature embedding. The input data can be represented as  $D = (G, X)$ . In the multi-modal setting, we assume  $m$  modalities as input and denote them as  $D = (G, (X_1, X_2, \dots, X_m))$ .

A crucial step in hypergraph learning is the construction of the hypergraph structure. To achieve this, we first obtain the feature embeddings  $X = \{X_1, X_2, \dots, X_m\}$  from the multi-modality data using a pre-trained network backbone, as illustrated in Fig. 1(b). We then employ a neighbor strategy in feature space to generate the hyperedge groups following the same protocol as described in [8]. Specifically, for each vertex, its  $k$ -nearest neighbors in the feature space are connected by a hyperedge, resulting in the set of hyperedges  $E_k = \{N_{\text{KNN}_k}(v) | v \in V\}$ . These hyperedge groups are concatenated together to form a hypergraph for each modality data. To effectively utilize the multi-modality knowledge, we concatenate  $k$  different hypergraphs to generate the final hypergraph by  $H = H_1 \| H_2 \| \dots \| H_k$ . Then, we feed the resulting data  $D$  into a Hypergraph Convolution Layer for further computation.

**Hypergraph Convolution.** We use spatial hypergraph convolution layers [8] for message aggregation. Messages can be passed either from vertex to hyperedge or from hyperedge to vertex using hyperpaths  $P$ , which is defined as  $P(v_1, v_k) = (v_1, e_1, v_2, \dots, e_{k-1}, v_k)$ . We define the inter-neighbor relation  $N$  of hypergraph  $G$  as  $N = \{(v, e) | w_{v,e} = 1, v \in V, \text{ and } e \in E\}$ . The vertex inter-neighbor set of hyperedge  $e$  is defined as  $N_v(e) = \{v | vNe\}$ , and the hyperedge inter-neighbor set of vertex  $v$  is defined as  $N_e(v) = \{e | vNe\}$ . To update the vertex information, we aggregate the messages from its hyperedge inter-neighbors  $N_e(v)$ , and to update the hyperedge information, we use the vertex inter-neighbors  $N_v(e)$ . Thus, the spatial hypergraph convolution layer is defined as

$$f_e = \sum_{v \in N_v(e)} h_{v,e} \cdot \frac{x_v}{|N_v(e)|}, \quad f'_v = \sigma \left( \sum_{e \in N_e(v)} \frac{f_e}{|N_e(v)|} \cdot \Theta \right), \quad (1)$$

where  $x_v$ ,  $f_e$ , and  $f'_v$  are the input, hidden, and output feature vectors.  $\Theta$  is a trainable parameter of the current hypergraph convolution layer.  $\sigma$  is a non-linear activation function, such as ReLU. The two-step message aggregation realizes a closed message passing loop among vertices, which enables the model to capture higher-order relationships between the vertices in the hypergraph.

## 2.2 Hypergraph Information Bottleneck (HGIB)

To balance the expressiveness and robustness of the model, we aim to optimize the vertex representation to capture the minimal sufficient information required for downstream tasks via the information bottleneck approach [25]. The Hypergraph Information Bottleneck (HGIB) approach, as shown in Fig. 1(a), is derived from the Graph Information Bottleneck [27], which requires the node representation  $Z_v$  to minimize the information from hypergraph-structured data  $D$  while maximizing the information to prediction  $Y$ . However, a major challenge in realizing HGIB numerically is the assumption of independent and identically distributed (IID) vertices, which is not feasible for many real-world scenarios. Therefore, we rely on a local dependence assumption for hypergraph-structured data, whereby given data related to a limited number of neighbors of vertex

$v$ , the data in the rest of the hypergraph is independent of  $v$ . We assume a Markovian dependence to obtain the optimal representation, whereby the representation of each vertex is updated by incorporating its neighbors with respect to the hypergraph representation  $X$ . The information bottleneck seeks to optimise

$$\min_{\mathbb{P}(Z^l|D) \in \Omega} \mathcal{L}_{\text{HGIB}}(X, Y; Z^l) := [-I(Y; Z^l) + \beta I(X; Z^l)], \quad (2)$$

where  $\Omega$  characterises the space of conditional distribution of  $Z^l$  given data  $D$ , and  $\beta$  is a balancing weight.  $l$  represents the  $l$ -th hypergraph convolution layer.

We now define the mutual information  $I(X; Z^l)$ , between the initial vertex embedding and updated vertex embedding, following [16]. This yield to the Cross-Entropy loss that reads:

$$I(Y; Z^l) \rightarrow - \sum_{v \in V} \text{CE}(Z_v^l W_{out}; Y_v), \quad (3)$$

where  $W_{out}$  is the weight of projector to predict the MCI conversion labels. We then assume that the elements in  $X^l$  are IID Bernoulli distributions:  $Z^l = \bigcup_{i,j} \{z_{i,j} \in \{0, 1\} | z_{i,j} \stackrel{i.i.d}{\sim} \text{Bernoulli}(0.5)\}$ . So the mutual information can be defined as  $I(X; Z^l) = \frac{1}{nm} \sum_{i=1}^n \sum_{j=1}^m \text{KL}(\text{Bernoulli}(z_{ij}^l) \parallel \text{Bernoulli}(0.5))$ . Here, KL denotes the Kullback-Leibler divergence between two Bernoulli distributions.

### 2.3 Optimisation Scheme

Our main task is MCI prediction conversion. This problem is taken from the perspective of a three class prediction task (NC, MCI, and AD). We have as basis a cross-entropy loss for classification. In the medical domain, it is usual to encounter with the class imbalance problem. To address this issue, we incorporate a focal loss. We then define our overall optimisation scheme as

$$\mathcal{L}_{total} = \frac{1}{|V|} \sum_{v \in V} \left\{ \text{CE}(P_v; Y_v) + \mu [-\alpha(1 - P_v)^\gamma \log(P_v)] \right\} + \xi \frac{1}{L} \sum_{l=1}^L \mathcal{L}_{\text{HGIB}}, \quad (4)$$

where  $\mu$  and  $\xi$  are balancing parameters.  $\alpha$  and  $\gamma$  are two hyper-parameters for the focal loss [13] in our experiments, we set their values to 2 and 0.5 respectively.

## 3 Experimental Results

In this section, we describe in detail the set of experiments performed to validate our proposed HGIB framework for prognosis prediction of Alzheimer’s Disease.

### 3.1 Dataset Description

We conduct our evaluation on the Alzheimer’s Disease Neuroimaging Initiative (ADNI) dataset<sup>3</sup>. ADNI is a longitudinal multi-centre and multi-modality

<sup>3</sup> Data used in the preparation of this article were obtained from the Alzheimer’s Disease Neuroimaging Initiative (ADNI) database ([adni.loni.usc.edu](http://adni.loni.usc.edu)).

study designed for the early detection and tracking of Alzheimer’s disease. The dataset contains four categories: Normal Control (NC), early Mild Cognitive Impairment (EMCI), late Mild Cognitive Impairment (LMCI), and Alzheimer’s disease (AD) at the Baseline Visit while only three categories afterwards: NC, Mild Cognitive Impairment (MCI), and AD. We focus on patients diagnosed with MCI (EMCI/LMCI) at the baseline visit. The goal is to predict the diagnosis of MCI conversion within a fixed two-year window to identify whether subjects converted to NC and AD or not, based on the multi-modality data including MRI, PET, and Non-imaging information. The Non-imaging information consists of demographic, genetic, and cognitive features, *e.g.*, age, gender, education, APOE4, MMSE, ADNI-MEM [4], ADNI-EF [9]. After the filter, we got 248 patients with complete three modalities from ADNI-2.

### 3.2 Dataset Pre-processing

For the data pre-processing, all MRI volumes are processed following (1) anterior commissure (AC)-posterior commissure (PC) alignment, (2) skull stripping, (3) intensity correction, (4) cerebellum removal, and (5) linear alignment to a template MRI. The corresponding PET volumes are aligned to their MRI volume via linear registration. For the Non-imaging data, we normalise each feature in the range of [0,1] before feeding them into the network.

### 3.3 Evaluation Protocol

We discuss the following conditions in our experiments: (1) the classification accuracy of HGIB compared with state-of-the-art hypergraph neural network methods; (2) performance comparison under different label counts of our method vs. existing techniques; (3) robustness analysis under two kinds of attacks. We follow standard protocol in the medical domain and use the area under the ROC curve (AUC), Positive predictive value (PPV %), and negative predictive value (NPV %) to measure the performance. For the results, we report the average performance and standard deviation over five independent runs.

We implemented our framework using PyTorch [18] and DHG<sup>4</sup> library on one NVIDIA A100 GPU. Our framework was optimised with the Adam algorithm for 2,000 epochs. The learning rate was set as  $1 \times 10^{-4}$  and decreased to 0. We set the number of neighbours as 20 when constructing the hypergraph. We empirically set the hyper-parameters  $\mu$  and  $\xi$  as 1 and 10 respectively.

### 3.4 Results & Discussion

**Comparison to Other Hypergraph Neural Networks.** We start evaluating our framework against three state-of-the-art hypergraph neural networks. HGNN [7] is a hypergraph neural network based on spectral convolution. DHGNN [12] exploits dynamically updating hypergraph structure on each layer. While

<sup>4</sup> <https://deephpergraph.com>

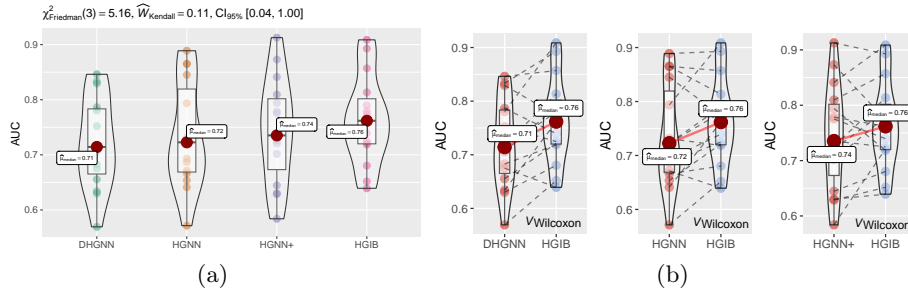


**Fig. 2.** Statistical analysis of our technique vs. existing ones. (a) Displays a outcome of the non-parametric Friedman test. (b) Displays pair-wise comparison performed using the Wilcoxon test.

**Table 1.** Comparison of our method (HGIB) and existing hypergraph techniques. The top results are highlighted in **bold**.

Methods	AUC			AUC average	PPV average	NPV average
	NC	MCI	AD			
DHGNN [12]	0.6437 ± 0.08	0.5546 ± 0.09	0.6841 ± 0.11	0.6275	50.88	69.89
HGNN [7]	0.7114 ± 0.02	0.6407 ± 0.04	<b>0.8516 ± 0.03</b>	0.7346	<b>63.49</b>	74.37
HGNN+ [8]	0.7454 ± 0.04	0.6532 ± 0.07	0.8325 ± 0.07	0.7437	55.07	74.03
<b>HGIB (Ours)</b>	<b>0.7504 ± 0.03</b>	<b>0.6789 ± 0.03</b>	0.8492 ± 0.05	<b>0.7595</b>	60.98	<b>76.19</b>

HGNN+ [8] is an extended version of HGNN which is a general high-order multi-modal data correlation modelling framework.

We report the quantitative comparison of our technique vs. existing techniques in Table 1. In a closer look at this table, we observe that our HGIB framework reports the best AUC performance on NC and MCI categories and best average AUC and NPV results. And the AUC performance of AD generates the comparable performance (0.8492) to the top value (0.8516). The highest NPV value of 76.19% also indicates that HGIB is more reliable to identify true negative cases and avoiding false negatives. Across all the results, our framework demonstrates that utilising the information bottleneck can further improve the network prognosis prediction ability. To further support our experimental results, we ran set of statistical tests. Firstly, we ran a non-parametric test for multiple comparisons. In particular, we use the Friedman test along with the Kendall’s coefficient of concordance with 95% confidence intervals as measure of the effect size for the Friedman test. The results are displayed in Fig. 2(a). We can then conclude that there is a significant difference in performance  $\chi^2_{Friedman}(3) = 5.16$ . The effect size  $W_{Kendall} = 0.11$  with 95% CI. We then performed a pair-wise comparison using the non-parametric Wilcoxon test yielding to  $V_{Wilcoxon} = 17.50, 30, 40$  for DHGNN vs. HGIB, HGNN vs. HGIB and HGNN+ vs. HGIB, respectively.

**Performance Comparison over Different Label Counts.** To demonstrate the effectiveness of our proposed method with limited labelled data, we

**Table 2.** Comparison of our method (HGIB) and existing hypergraph techniques under different training sample settings. The top results are highlighted in **bold**.

Methods	80%			60%			40%		
	AUC	PPV	NPV	AUC	PPV	NPV	AUC	PPV	NPV
DHGNN [12]	0.7208	56.08	73.71	0.6981	53.20	71.43	0.6911	47.05	72.75
HGNN [7]	0.7346	<b>63.49</b>	74.37	0.7300	55.60	74.68	0.7282	58.84	75.51
HGNN+ [8]	0.7437	55.07	74.03	0.7425	55.51	74.71	0.7162	55.90	73.62
<b>HGIB (Ours)</b>	<b>0.7595</b>	60.98	<b>76.19</b>	<b>0.7443</b>	<b>57.93</b>	<b>76.63</b>	<b>0.7393</b>	<b>60.81</b>	<b>76.22</b>

**Table 3.** Robustness Analysis. The top results are highlighted in **bold** font.

Methods	Attack	AUC	Attack	AUC	Attack	AUC
HGNN+ [8]	-	0.7437 $\pm$ 0.05	Drop	0.7155 $\pm$ 0.02	Noise	0.7061 $\pm$ 0.04
<b>HGIB (Ours)</b>	-	<b>0.7595 <math>\pm</math> 0.02</b>	Drop	<b>0.7452 <math>\pm</math> 0.02</b>	Noise	<b>0.7326 <math>\pm</math> 0.01</b>

conducted experiments with three different label counts (80%, 60%, and 40% of training patients). The results are reported in Table 2, which shows that HGIB outperforms all compared techniques. We also observed that even when trained with fewer annotated data samples, our method still achieved good performance with a slight decrease compared to the full set of annotated data. This suggests that HGIB can effectively learn from limited data and generalize well to the remaining testing data by identifying relevant information (*e.g.*, features and patterns), thus improving prognosis prediction.

**Robustness Analysis under Attacks.** To study the robustness of the proposed HGIB under the hypergraph topology and feature tasks, we conduct experiments by (1) randomly drop 20% hyperedges from the original hypergraph for structure attack; (2) randomly inject feature noise to the extracted feature embedding  $X$  for feature attack. Specifically, we define the mean of the maximum value of each vertex feature as  $r$ , random Gaussian noise as  $\epsilon \sim N(0, 1)$ , and feature noise ratio as  $\rho$ . We then calculate noise according to  $\eta = \rho \cdot r \cdot \epsilon$ . We set  $\rho$  as 0.01 in the experiments. The results are shown in Table 3. The results, shown in Table 3, demonstrate that HGIB consistently outperforms the previous state-of-the-art HGNN+ [8] in both scenarios, indicating that HGIB enhances the model’s robustness for structure and feature perturbations, supporting its effectiveness for generalization and robustness.

## 4 Conclusion

Our proposed HGIB demonstrated promising results in addressing the challenges associated with Alzheimer’s disease prognosis leveraging multi-modal data. By utilising a hypergraph structure to represent the multi-modal features and enforcing learning discriminative representations with the help of the principle of information bottleneck, HGIB outperforms other state-of-the-art hypergraph

neural network architectures in supervised learning settings and under fewer annotations. Our results also demonstrated better robustness of HGIB under both topological and feature perturbations. The success of HGIB highlights the potential of hypergraph-based methods in the field of Alzheimer’s disease prognosis prediction and sets a foundation for future research in this area.

## 5 Acknowledgement

This work was supported by grants to: SW from Wellcome Trust 221633/Z/20/Z; AIAR from CMIH and CCIMI, University of Cambridge; ZK acknowledges support from the Biotechnology and Biological Sciences Research Council H012508 and BB/P021255/1, Alan Turing Institute TU/B/000095, Wellcome Trust 205067/Z/16/Z, 221633/Z/20/Z, Royal Society INF/R2/202107; CBS from the Philip Leverhulme Prize, the Royal Society Wolfson Fellowship, the EPSRC advanced career fellowship EP/V029428/1, EPSRC grants EP/S026045/1 and EP/T003553/1, EP/N014588/1, EP/T017961/1, the Wellcome Innovator Awards 215733/Z/19/Z and 221633/Z/20/Z, the European Union Horizon 2020 research and innovation programme under the Marie Skłodowska-Curie grant agreement No. 777826 NoMADS, the Cantab Capital Institute for the Mathematics of Information and the Alan Turing Institute.

## References

1. Aviles-Rivero, A.I., Runkel, C., Papadakis, N., Kourtzi, Z., Schönlieb, C.B.: Multi-modal hypergraph diffusion network with dual prior for alzheimer classification. In: Medical Image Computing and Computer Assisted Intervention–MICCAI 2022: 25th International Conference, Singapore, September 18–22, 2022, Proceedings, Part III. pp. 717–727. Springer (2022)
2. Bae, J., Stocks, J., Heywood, A., Jung, Y., Jenkins, L., Hill, V., Katsaggelos, A., Popuri, K., Rosen, H., Beg, M.F., et al.: Transfer learning for predicting conversion from mild cognitive impairment to dementia of alzheimer’s type based on a three-dimensional convolutional neural network. *Neurobiology of aging* **99**, 53–64 (2021)
3. Costafreda, S.G., Dinov, I.D., Tu, Z., Shi, Y., Liu, C.Y., Kloszewska, I., Mecocci, P., Soininen, H., Tsolaki, M., Vellas, B., et al.: Automated hippocampal shape analysis predicts the onset of dementia in mild cognitive impairment. *Neuroimage* **56**(1), 212–219 (2011)
4. Crane, P.K., Carle, A., Gibbons, L.E., Insel, P., Mackin, R.S., Gross, A., Jones, R.N., Mukherjee, S., Curtis, S.M., Harvey, D., et al.: Development and assessment of a composite score for memory in the alzheimer’s disease neuroimaging initiative (ADNI). *Brain imaging and behavior* **6**, 502–516 (2012)
5. Davatzikos, C., Bhatt, P., Shaw, L.M., Batmanghelich, K.N., Trojanowski, J.Q.: Prediction of MCI to AD conversion, via MRI, CSF biomarkers, and pattern classification. *Neurobiology of aging* **32**(12), 2322–e19 (2011)
6. Fan, Y., Resnick, S.M., Wu, X., Davatzikos, C.: Structural and functional biomarkers of prodromal alzheimer’s disease: a high-dimensional pattern classification study. *Neuroimage* **41**(2), 277–285 (2008)

7. Feng, Y., You, H., Zhang, Z., Ji, R., Gao, Y.: Hypergraph neural networks. In: Proceedings of the AAAI conference on artificial intelligence. vol. 33, pp. 3558–3565 (2019)
8. Gao, Y., Feng, Y., Ji, S., Ji, R.: HGNN+: General hypergraph neural networks. *IEEE Transactions on Pattern Analysis and Machine Intelligence* (2022)
9. Gibbons, L.E., Carle, A.C., Mackin, R.S., Harvey, D., Mukherjee, S., Insel, P., Curtis, S.M., Mungas, D., Crane, P.K., Initiative, A.D.N.: A composite score for executive functioning, validated in alzheimer’s disease neuroimaging initiative (ADNI) participants with baseline mild cognitive impairment. *Brain imaging and behavior* **6**, 517–527 (2012)
10. Grueso, S., Viejo-Sobera, R.: Machine learning methods for predicting progression from mild cognitive impairment to alzheimer’s disease dementia: a systematic review. *Alzheimer’s research & therapy* **13**, 1–29 (2021)
11. Hansson, O., Zetterberg, H., Buchhave, P., Londos, E., Blennow, K., Minthon, L.: Association between CSF biomarkers and incipient alzheimer’s disease in patients with mild cognitive impairment: a follow-up study. *The Lancet Neurology* **5**(3), 228–234 (2006)
12. Jiang, J., Wei, Y., Feng, Y., Cao, J., Gao, Y.: Dynamic hypergraph neural networks. In: *IJCAI*. pp. 2635–2641 (2019)
13. Lin, T.Y., Goyal, P., Girshick, R., He, K., Dollár, P.: Focal loss for dense object detection. In: Proceedings of the IEEE international conference on computer vision. pp. 2980–2988 (2017)
14. Liu, Y., Yue, L., Xiao, S., Yang, W., Shen, D., Liu, M.: Assessing clinical progression from subjective cognitive decline to mild cognitive impairment with incomplete multi-modal neuroimages. *Medical image analysis* **75**, 102266 (2022)
15. McEvoy, L.K., Fennema-Notestine, C., Roddey, J.C., Hagler Jr, D.J., Holland, D., Karow, D.S., Pung, C.J., Brewer, J.B., Dale, A.M.: Alzheimer disease: quantitative structural neuroimaging for detection and prediction of clinical and structural changes in mild cognitive impairment. *Radiology* **251**(1), 195–205 (2009)
16. Nguyen, X., Wainwright, M.J., Jordan, M.I.: Estimating divergence functionals and the likelihood ratio by convex risk minimization. *IEEE Transactions on Information Theory* **56**(11), 5847–5861 (2010)
17. Pan, X., Phan, T.L., Adel, M., Fossati, C., Gaidon, T., Wojak, J., Guedj, E.: Multi-view separable pyramid network for AD prediction at MCI stage by 18 F-FDG brain PET imaging. *IEEE Transactions on Medical Imaging* **40**(1), 81–92 (2020)
18. Paszke, A., Gross, S., Massa, F., Lerer, A., Bradbury, J., Chanan, G., Killeen, T., Lin, Z., Gimelshein, N., Antiga, L., Desmaison, A., Kopf, A., Yang, E., DeVito, Z., Raison, M., Tejani, A., Chilamkurthy, S., Steiner, B., Fang, L., Bai, J., Chintala, S.: PyTorch: An imperative style, high-performance deep learning library. In: *Advances in Neural Information Processing Systems* 32, pp. 8024–8035. Curran Associates, Inc. (2019)
19. Qiu, A., Fennema-Notestine, C., Dale, A.M., Miller, M.I., Initiative, A.D.N., et al.: Regional shape abnormalities in mild cognitive impairment and alzheimer’s disease. *Neuroimage* **45**(3), 656–661 (2009)
20. Risacher, S.L., Saykin, A.J., Wes, J.D., Shen, L., Firpi, H.A., McDonald, B.C.: Baseline MRI predictors of conversion from MCI to probable AD in the ADNI cohort. *Current Alzheimer Research* **6**(4), 347–361 (2009)
21. Shaw, L.M., Vanderstichele, H., Knapik-Czajka, M., Clark, C.M., Aisen, P.S., Petersen, R.C., Blennow, K., Soares, H., Simon, A., Lewczuk, P., et al.: Cerebrospinal

- fluid biomarker signature in alzheimer’s disease neuroimaging initiative subjects. *Annals of neurology* **65**(4), 403–413 (2009)
22. Shen, H.T., Zhu, X., Zhang, Z., Wang, S.H., Chen, Y., Xu, X., Shao, J.: Heterogeneous data fusion for predicting mild cognitive impairment conversion. *Information Fusion* **66**, 54–63 (2021)
  23. Shigemizu, D., Akiyama, S., Higaki, S., Sugimoto, T., Sakurai, T., Boroevich, K.A., Sharma, A., Tsunoda, T., Ochiya, T., Niida, S., et al.: Prognosis prediction model for conversion from mild cognitive impairment to alzheimer’s disease created by integrative analysis of multi-omics data. *Alzheimer’s Research & Therapy* **12**, 1–12 (2020)
  24. Syaifullah, A.H., Shiino, A., Kitahara, H., Ito, R., Ishida, M., Tanigaki, K.: Machine learning for diagnosis of AD and prediction of MCI progression from brain MRI using brain anatomical analysis using diffeomorphic deformation. *Frontiers in Neurology* **11**, 576029 (2021)
  25. Tishby, N., Pereira, F.C., Bialek, W.: The information bottleneck method. arXiv preprint physics/0004057 (2000)
  26. Toussaint, P.J., Perlberg, V., Bellec, P., Desarnaud, S., Lacomblez, L., Doyon, J., Habert, M.O., Benali, H., et al.: Resting state FDG-PET functional connectivity as an early biomarker of alzheimer’s disease using conjoint univariate and independent component analyses. *Neuroimage* **63**(2), 936–946 (2012)
  27. Wu, T., Ren, H., Li, P., Leskovec, J.: Graph information bottleneck. *Advances in Neural Information Processing Systems* **33**, 20437–20448 (2020)
  28. Zhu, Y., Kim, M., Zhu, X., Kaufer, D., Wu, G., Initiative, A.D.N., et al.: Long range early diagnosis of alzheimer’s disease using longitudinal MR imaging data. *Medical image analysis* **67**, 101825 (2021)